Magnetic ordered phase in La$_{0.6}$Sr$_{0.4}$MnO$_3$ ferromagnets

L. B. Steren,* M. Sirena, and J. Guimpel

Centro Atómico Bariloche and Instituto Balseiro, Comisión Nacional de Energía Atómica, 8400 S. C. de Bariloche, R. N., Argentina
(Received 8 July 2001; published 20 February 2002)

The ferromagnetic phase of La$_{0.6}$Sr$_{0.4}$MnO$_3$ thin films has been investigated through measurements of magnetization loops at different temperatures, zero-field-cooled and field-cooled magnetization curves obtained under different magnetic fields. We have found that the main sources of the ''bulk'' coercivity in manganite films are the film/substrate interface and film surface. The temperature dependence of the coercivity is described by a ''strong domain-wall pinning'' model, independently of the thickness and substrate. The magnetization-vs-temperature curves, measured under different magnetic fields (10 Oe$<H<$2.5 kOe), have been explained in terms of the magnetic hysteresis of the films. We find no evidence of glass states or of the existence of single-domain clusters, as suggested by other authors.

I. INTRODUCTION

In recent years, manganite oxides have attracted a lot of attention due to their potential application as magnetoresistive sensors. $A_{1-x}B_x$MnO$_3$ ($A=$La, $B=$Sr,Ba,Ca) compounds exhibit a wide variety of magnetic and electric transport properties, depending on the concentration x.[1] In the region $0.2<x<0.5$ these compounds present ferromagnetic order and an insulator-metal transition near the Curie temperature, while the undoped parent compound LaMnO$_3$ is an antiferromagnetic insulator. Zenner[2] proposed the existence of a double-exchange interaction between Mn^{3+} and Mn^{4+} to explain both the ferromagnetic order and the metallic character of the doped compounds. Many questions have been opened about the interplay of this ferromagnetic term with the antiferromagnetic superexchange in manganite compounds. de Gennes[3] proposed the existence of a frustrated phase in an intermediate-concentration range, based on the competition between both interactions. The important magnetohistory effect observed in the ferromagnetic manganites has given rise to a wide variety of interpretations for the magnetic phases of these compounds.[4,5] Ju and Sohn discuss in Ref. 4 zero-field-cooled (ZFC) and field-cooled (FC) magnetization curves and the thermal dependence of coercitivity in terms of spin freezing and magnetic inhomogeneity. These authors studied the variation of the magnetization curves with oxygen content of different bulk and film samples of La-Ca-Mn-O and La-Ba-Mn-O, and interpreted their results in the frame of a ''spin-clustered'' system. As these compounds are highly disordered, with Mn^{3+}-Mn^{4+} pairs distributed randomly, the idea of clusters embedded in a non-magnetic matrix has been introduced for the explanation of some experimental results. However, the temperature dependence of the coercive field does not follow the expected law for blocked cluster systems. Moreover, the blocking temperature deduced from the fit does not correspond to the maximum in the ZFC curves. Li and coworkers[5] introduced the concept of a ''cluster-glass'' phase in La$_{0.7}$Sr$_{0.3}$Mn$_{0.7}$Co$_{0.3}$O$_3$. In spite of the fact that for Co doping the interpretation of the experimental data is complicated due to the coexistence of Co in different electronic states, the features observed in magnetization measurements and attributed to a field-induced transition from a cluster-glass to a ferromagnetic phase could not be taken as conclusive on this subject. It is important to remark that irreversibilities between zero-field-cooled and field-cooled magnetization curves have been observed in both ferromagnetic bulk[5,6] and film samples,[4] so they cannot be only assigned to substrate influence on the magnetic properties.

We believe that without performing a complete experimental study of the magnetism of the samples it is rather difficult to identify complex magnetic phases, like spin or cluster glasses. In this work, the field and temperature dependences of the magnetization of magnetoresistive La$_{0.6}$Sr$_{0.4}$MnO$_3$ thin films have been studied for different magnetic histories in order to understand the nature of the magnetic order in these compounds. Bulk La$_{1-x}$B$_x$MnO$_3$ ($0.2<x<0.5$; B:Sr,Ba,Ca) is a relatively soft material [$H_c \leq 10$ Oe (Ref. 7)]. Due to the fact that ''low-field'' magnetic measurements are usually performed in fields larger than 10 Oe, small magnetohistory effects have been reported for bulk compounds. However, in thin films, the coercive field is larger[8] and a rich variety of behaviors is observed, depending on the applied field and temperature.

II. EXPERIMENTAL DETAILS

The films were grown by dc magnetron sputtering from a stoichiometric ceramic target of nominal composition La$_{0.6}$Sr$_{0.4}$MnO$_3$ (LSMO). Films with thickness t, ranging from 5 nm to 500 nm, were grown both on (100) MgO and (100) SrTiO$_3$ single-crystalline substrates. The growth temperature was 660° C. After deposition the film was cooled down slowly to room temperature in a 100 Torr O$_2$ partial pressure.

The film composition was measured by energy dispersive x-ray analysis (EDAX). The results show that the composition of the films is that of the target within 10% and that it is homogeneous along the sample. The crystalline structure of the samples was characterized by x-ray diffraction spectroscopy. X-ray diffraction patterns indicate that the films are strongly textured, with the (001) pseudocubic axis in the film normal direction.[9] The lattice-parameter-thickness dependence shows evidence of strains, for SrTiO$_3$ (STO) sub-

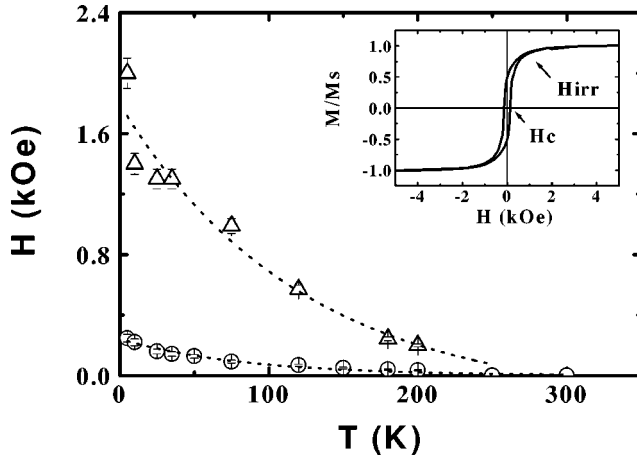FIG. 1. Temperature dependence of the coercivity (open circles) and the irreversible field (open triangles), respectively, for a LSMO/MgO film of $t=240$ nm. Inset: hysteresis loop of the same sample, measured at 50 K. The characteristic fields H_c and H_{irr} are identified by arrows. Dotted lines are guides to the eye.

FIG. 2. Coercitivity as a function of film thickness t for (solid circles) LSMO-MgO and (solid triangles) LSMO-STO films, respectively. The solid lines are fits of Eq. (1) to the data.

strates, and decoupled growth for MgO substrates.

The magnetic measurements were performed in a commercial superconducting quantum interference device (SQUID) magnetometer. Hysteresis loops were measured at different temperatures between 5 K and 300 K for fields up to 5 T. Zero-field-cooled and field-cooled magnetization curves were measured in applied magnetic fields H, ranging from 10 Oe to 2.5 kOe. The procedure for these measurements was the following: for ZFC curves, a virgin sample is cooled down to 5 K. Once the temperature is stable, the magnetic field is applied and the measurement started. There is always a time delay between two consecutive data points, needed to stabilize the temperature.

III. RESULTS AND DISCUSSION

A. Temperature dependence of the hysteresis loops

Magnetization-vs-temperature curves[10] show that the films order ferromagnetically around 240 K. The Curie temperature depends on the substrate and the thickness of the films: it decreases with film thickness, notably for t <100 nm. The inset of Fig. 1 shows the field dependence of the magnetization, measured below the Curie point, for a LSMO/MgO film of $t=240$ nm. The substrate contribution has been subtracted from the raw data.[11] The loops are elongated and close at H_{irr}, a field that is considerably higher than the coercivity, H_c.

The coercive field is thickness and substrate dependent. Lower coercivities were systematically observed in films grown on SrTiO₃, in comparison to those measured in the LSMO-MgO series. In both cases, the coercivity decreases as the thickness increases. We qualitatively describe this behavior by a linear dependence (see Fig. 2):
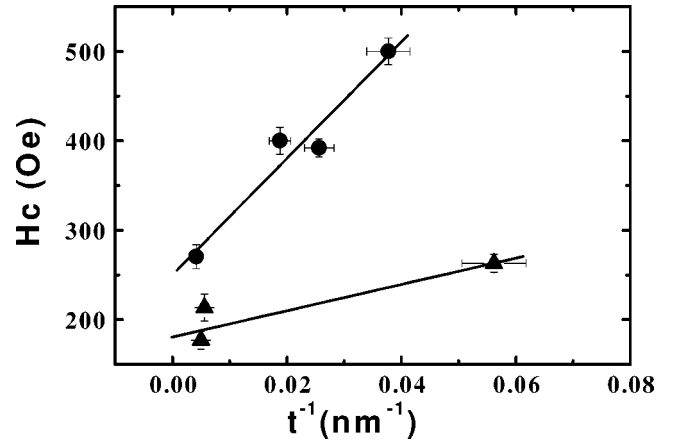
$$H_{c0}=H_{cb0}+\frac{P_0}{t}, \quad (1)$$

where H_{cb0} is the extrapolated "bulk" coercivity and P_0 a constant that depends on the film substrate and growth conditions. For $T=5$ K, the "bulk" coercivity is 240(10) Oe for the MgO series and 180(10) Oe for the STO one. These values are notably higher than those measured in bulk samples, typically smaller than 10 Oe. This discrepancy can be mainly attributed to the important difference of the volume anisotropy constants measured in bulk and thin film samples.[8]

The P_0 constant is 6500(200) Oe nm for the LSMO-MgO films and 1300(400) Oe nm for the LSMO-STO films, respectively. The thickness dependence of the coercivity could be attributed to the film surface and film/substrate (F/S) interface. It has been demonstrated theoretically and measured in different systems[12] that surface roughness introduces barriers for the domain-wall motion, increasing the coercivity of the films. S/F interfacial coercivity arises from lateral variations in the domain-wall (DW) energy, originated in local strains, variation of exchange stiffness, or anisotropy, etc.[12] Antiferromagnetic (AFM) measurements show that the surface roughness is similar in all our samples.[9] The average amplitude of the surface roughness is 2 nm with a mean wavelength of 80 nm.[13] Therefore, the difference between the P_0 constant of LSMO-MgO and LSMO-STO samples cannot be explained by surface irregularities. We attribute our results mainly to S/F effects. As was commented above, the growth mode of the two series of samples is different: While the LSMO-MgO films accommodate the lattice mismatch in a transient layer of $t_l<100$ nm with structural defects (strains, dislocations, and point defects), the LSMO-STO films grow epitaxially in a strained lattice. The lattice strains relax along the sample but are still noticeable in the thicker films.[9]

Measurements of the temperature variation of the coercivity are used to identify the mechanism responsible for it and to obtain insight into the properties of the pinning centers. In Fig. 1, the temperature dependence of the coercivity and of H_{irr} for a LSMO-MgO film is shown. It can be seen that both H_c and H_{irr} fall off rapidly with temperature, becoming zero around room temperature. Previous domain imaging ex-
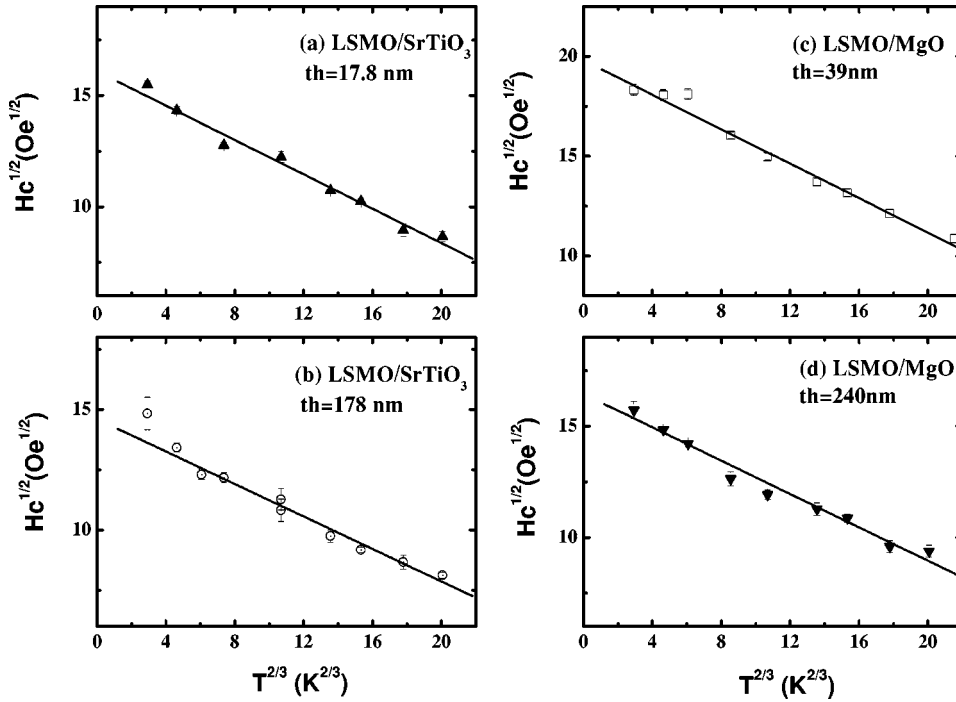
FIG. 3. Temperature dependence of the coercive field for different LSMO films. Solid lines are the best fits of the data using the SDWP model.

periments performed on epitaxial LSMO films[14] reveal that magnetization changes occur by rotation and DW movement over large areas.

Domain-wall pinning by inhomogeneities has been proposed by many authors as a source of magnetic hardening. The usual assumption is that the walls bow out between individual pinning sites and escape when the applied magnetic field, aided by thermal activation, reaches a critical value. In general, DW's interact with a great number of defects. A statistical theory of the temperature dependence of the coercivity has been proposed by Gaunt,[15] based on the interaction between DW's and pin sites. A distinction between "strong" and "weak" DW pinning is made in the model. The strong- and weak-pinning models differ significantly in the prediction concerning the activation energy required to unpin a wall. In weak domain-wall pinning, the walls break away cooperatively from many pinning sites in the coercive field. Thermal excitation leads to a linear decrease of the coercive field with temperature. On the other hand, in the limit of "strong-DW-pinning" (SDWP), the domain walls are strongly pinned by obstacles bowing out before breaking away from a pin, before interacting with another one. In this case, the coercivity varies with temperature as $T^{3/2}$. A work performed by Gaunt and Mylvaganam[16] showed that thermally activated escape of DW's from continuous planar pin sites is also possible. These authors proved that the formation of blisters in the walls pinned along the planar defect allows the thermal activation of the DW's from these pinning sites. For this case, the authors derived an expression for the coercivity, which depends linearly on temperature.

We have studied our results within the framework of these models. The fits have been made in the low-temperature region, where small changes of magnetization and anisotropy are observed (less than 4%),[8,10] while a variation of around 60% is measured in the coercivity. For these characteristics,

the temperature dependence of the coercivity can be attributed mainly to domain-wall movement or rotation.

It is evident from Fig. 1 that the temperature dependence of the coercivity does not follow a linear law. The existence of continuous planar pinning sites or a "weak-domain-wall-pinning regime" of random inhomogeneities is thus discarded. The same functional dependence has been found for the thermal variation of the coercivity in all the samples, independently of their substrate and thickness. The best fit was obtained using the SDWP model in the temperature range from 5 to 100 K (see Fig. 3). The coercivity varies with temperature as

$$H_c^{1/2} = Hc_0^{1/2}(1 - CT^{2/3}),\qquad(2)$$

with $C = (75k_b/4bf)^{2/3}$, where $4b$ is the wall width, f is the maximum restoring force a single pin can exert on a domain-wall segment, and k_b is the Boltzmann constant.

No significant change of C with the substrate or the film thickness is found. Assuming a domain-wall width of 30 nm, estimated from exchange and anisotropy constants data,[8,17] a restoring force of around 2×10^{-6} Dy is calculated. The pin densities, deduced from Hc_0, vary from 1.5×10^{15} cm^{-3} (estimated for the LSMO-STO films and thick LSMO-MgO films) to 9×10^{15} cm^{-3} in the thinner MgO-based films.

Our results show that the main domain-wall pinning mechanism present in manganite films can be modeled as a random array of inhomogeneities. The manganite compound is intrinsically disordered, due to the random cation substitution and consequent variation of Mn valence and localized lattice distortions. Together with probable "bulk" pinning centers, we should point out that the existence of stresses, dislocation planes, and point defects of the films may add
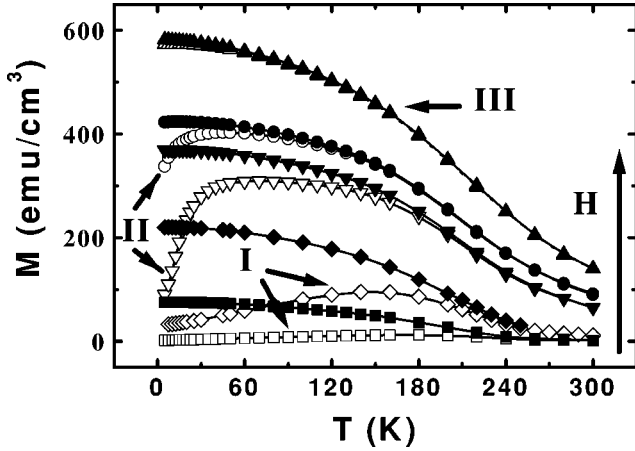
FIG. 4. ZFC (open symbols) and FC (solid symbols) magnetization curves, measured at different magnetic fields: (up triangles) 2.5 kOe, (circles) 0.5 kOe, (down triangles) 0.25 kOe, (diamonds) 57 Oe, and (squares) 19 Oe for a LSMO/MgO film of $t=240$ nm are shown. Solid lines are guides to the eye.

other pinning sites of different characteristics and behavior from the bulk ones and proper to this family of nanostructures.

B. Zero-field-cooled and field-cooled magnetization

Zero-field-cooled and field-cooled magnetizations, measured at different fields, are shown in Fig. 4. The field dependence of the ZFC curve as well as the irreversibility between ZFC and FC curves is strongly correlated with the hysteresis of the materials, as will be shown below. The irreversibility between ZFC and FC curves disappears above T_{irr}. In Fig 5, $(M_{FC}-M_{ZFC})/M_{FC}$ and T_{irr} are plotted as a function of magnetic field. The irreversibility and T_{irr} monotonically decrease with an increasing field in the whole field range. However, a rapid drop of both parameters is observed for fields smaller than the coercive field. Above this field and
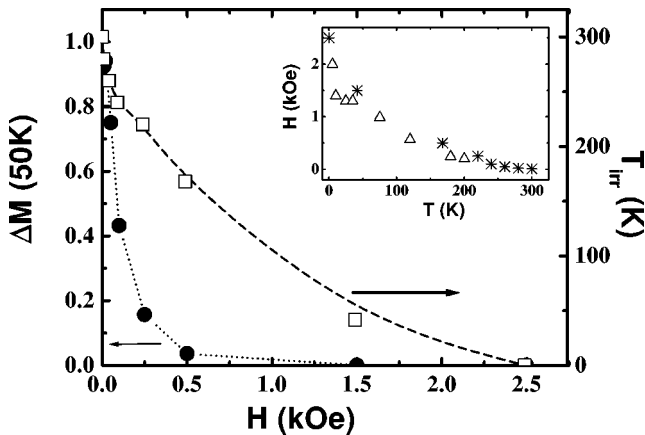

FIG. 5. Field dependence of (solid circles) $\Delta M=(M_{FC}-M_{ZFC})/M_{FC}$, measured at 50 K and (open squares) T_{irr} for a LSMO/MgO film of $t=240$ nm. The dashed and the dotted lines are guides to the eye. Inset: (stars) applied magnetic field H vs T_{irr} and (open triangles) H_{irr} vs T for the same sample.

up to H_{irr} the decay is slower. The ZFC and FC curves are merged into a single one above H_{irr}. These results can be understood in terms of the irreversibility of the magnetization loop. In agreement with hysteresis loops, irreversibility effects are only observed below H_{irr}, where domain movements take place. However and in spite of the fact that there are still irreversibilities between increasing and decreasing field magnetization curves up to H_{irr}, the larger effects are noticed for $H<H_c$, as observed in the ZFC-FC curves. As shown in the inset of Fig. 5, there is a direct equivalence of T_{irr} data extracted from ZFC-FC curves measured at fixed magnetic field H, and the H_{irr} data obtained from hysteresis loops measured at fixed temperature.

Three different shapes of ZFC curves have been observed, corresponding to different ranges of applied magnetic fields (Fig. 4). For fields $H<H_c$ (zone I), a broad maximum is observed close to the ordering temperature. The position of this maximum is shifted to lower temperatures as H increases. A wide variety of systems, such as spin glasses, single-domain particle assemblies, etc., present a maxima in ZFC curves. This is why several authors have attributed this feature to complex phases.[4,5] However, at fields much lower than the coercivity, the initial susceptibility of a ferromagnet monotonically increases with temperature, passing through a maximum below T_C. This behavior is due to the fact that the permeability of ferromagnets is inversely proportional to both the anisotropy and the magnetostriction constants which approach zero around T_C.[18]

For $H_c<H<H_{irr}$ (zone II), the ZFC magnetization is characterized by an abrupt increase at low temperature, followed by a smooth evolution to a plateau before joining the FC curve at T_{irr}. The magnetization change at low temperature is maximum for fields close to H_c. This effect can be attributed to the maximum viscosity of magnetization changes found at the coercive field in manganite films.[19] In fact, the field dependence of the magnetic viscosity for multidomain ferromagnets has been calculated[20] and measured in several systems.[21] It has been found that the field dependence of the viscosity has a bell shape, centered at or close to the coercivity. Due to the particular sequence (see Sec. II) used in our M-vs-T measurements, the abrupt change of magnetization expected when measuring at fields close to H_c is expanded in a rather large temperature range.

For $H>H_{irr}$ (zone III) the ZFC and the FC curves are superimposed, saturating at low temperature at $Ms(0)$. As has been shown in the previous section, the magnetization loops close at H_{irr} and thus no magnetohistory effects are expected at fields higher than H_{irr}.

The FC curves saturate at low temperature to $M_{FC}(0)$. The shape of these curves does not change with the applied field but $M_{FC}(0)$ increases with H, saturating at $Ms(0)$ for $H>H_{irr}$, with $Ms(0)=g\mu_B S$, where g is the gyromagnetic value, μ_B the Bohr magneton, and S the average spin of the manganite compound. This behavior is that of an ordinary ferromagnet: a spin glass would not show a saturation of the magnetization in the frozen state for such low fields and right above H_{irr}.[22]

The three regimes discussed above for the ZFC-FC curves can be also identified if we define a characteristic tempera-
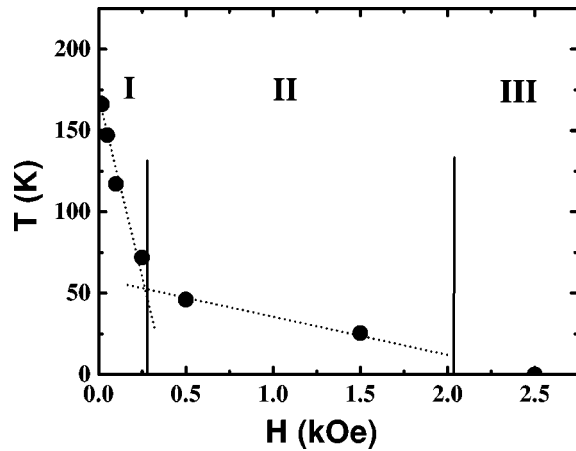
FIG. 6. Field dependence of T_{ZFC} for a LSMO/MgO film of t $=240$ nm ($H_C \sim 250$ Oe). The dotted lines are guides to the eye.

ture T_{ZFC} in the ZFC curves as $\partial M/\partial T|_{T_{ZFC}}=0$. In Fig. 6 the field dependence of T_{ZFC} for a LSMO film ($t=240$ nm) has been plotted. Due to the origin of the maximum of ZFC for low fields ($H\ll H_C$), no important variation of T_{ZFC} is expected for this field range. As H approaches $H_c(T=0)$, a rapid change of T_{ZFC} to lower temperature is observed (zone I). Afterwards, T_{ZFC} decreases smoothly between H_C and H_{irr} due to the decrease of the viscosity with field above H_c (zone II), approaching zero above H_{irr} as the system saturates (zone III).

The behavior described is similar for all samples independently of the film thickness or substrate. However, the characteristic fields H_c and H_{irr} and temperature T_{ZFC} do depend on thickness and substrate material.

IV. CONCLUSIONS

A detailed study of the magnetic properties of manganite films was performed in order to elucidate the nature of the magnetic ordered phase of these systems. A careful analysis of the experimental data was carried out, relating the field and temperature dependence of the magnetization of the samples, for different cooling conditions. Through the study of the thermal dependence of the coercivity the mechanism

responsible for domain-wall movement has been identified. A model of strong domain-wall pinning describes well the temperature dependence of the coercivity found in manganite films.

The temperature dependence of the ZFC and FC magnetization curves has been explained in terms of the hysteresis of these ferromagnetic materials. The irreversibility between ZFC and FC curves has been related to the hysteresis of the ferromagnet and thus to the domain structure of the samples. The variation of the shape of the ZFC curves has been associated with different stages of the magnetization of the sample. At very low fields, far from the coercivity, the magnetization presents a maximum below the Curie point related to the decrease to zero of the crystal anisotropy and magnetostriction near T_c. As the measuring field approaches the coercive field, a rapid increase of the magnetization is observed at low temperature, which has been asociated with the maximum of viscosity associated with magnetization changes near H_c. When the measuring field is higher than the coercivity, the difference between ZFC and FC curves becomes much smaller and decreases to zero for measuring fields $H > H_{irr}$. At high fields and low temperatures, both curves saturate at the expected value. We have shown that the ZFC and FC curves can be interpreted in terms of the close relationship existent between hysteresis loops and magnetic history of the samples. It has been shown that the relation between the measuring field and the characteristic fields of the hysteresis loop defines the shape of the ZFC curves. However, a quantitative analysis of the problem would be much more complicated due to the temperature dependence of these characteristic fields and the consequent effect on the magnetization of the system.

*Corresponding author. FAX: 54-2944-445299. Electronic address: steren@cab.cnea.gov.ar

[1] G.H. Jonker and J.H. Van Santen, Physica (Amsterdam) **16**, 337 (1950); J.H. Van Santen and G.H. Jonker, *ibid.* **16**, 599 (1950).

[2] C. Zener, Phys. Rev. **82**, 403 (1951).

[3] P.G. de Gennes, Phys. Rev. **118**, 141 (1960).

[4] H.L. Ju and H. Sohn, J. Magn. Magn. Mater. **167**, 200 (1997).

[5] X.-G. Li, X.J. Fan, G. Ji, W.B. Wu, K.H. Wong, C.L. Choy, and H.C. Ku, J. Appl. Phys. **85**, 1663 (1999).

[6] J. Mira, J. Rivas, F. Rivadulla, C. Vazquez-Vazquez, and M.A. Lopez-Quintela, Phys. Rev. B **60**, 2998 (1999).

[7] H. R. Salva (private communication).

[8] L.B. Steren, M. Sirena, and J. Guimpel, J. Appl. Phys. **87**, 6755 (2000).

[9] J. Guimpel, M. Sirena, and L.B. Steren, Thin Solid Films **373**, 102 (2000).

[10] L.B. Steren, M. Sirena, and J. Guimpel, J. Magn. Magn. Mater. **211**, 28 (2000).

[11] $\chi_s = \chi_d + \chi_{PM}$, where χ_d is the diamagnetic susceptibility of the substrate oxide and χ_{PM} corresponds to paramagnetic impurities of the substrate.

[12] M. Pardavi-Horvath, IEEE Trans. Magn. **21**, 1694 (1985) and references therein.

[13] The average substrate surface roughness as measured with AFM is 0.15(2) nm for MgO and 0.30(2) nm for STO. In both cases the mean lateral wavelength is of the order of 100 nm.

[14] A. Gupta, G.Q. Gong, G. Xiao, P.R. Duncombe, P. Lecoeur, P.

Trouilloud, Y.Y. Wang, V.P. Dravid, and J.Z. Sun, Phys. Rev. B **54**, 15 629 (1996).

[15] P. Gaunt, Philos. Mag. B **48**, 261 (1983).

[16] P. Gaunt and C.K. Mylvaganam, Philos. Mag. B **39**, 313 (1979).

[17] Y. Suzuki, H.Y. Hwang, S-W. Cheong, T. Siegrist, R.B. van Dover, A. Asamitsu, and Y. Tokura, J. Appl. Phys. **83**, 7064 (1998).

[18] A. Herpin, *Théorie du Magnétisme* (Presses Universitaires de France, Paris, France, 1968), pp. 808–815.

[19] M. Sirena, L.B. Steren, and J. Guimpel, Phys. Rev. B **64**, 104409 (2001).

[20] P. Gaunt, J. Appl. Phys. **59**, 4129 (1986).

[21] P. Rugkwawsook, C.E. Korman, G. Bertotti, and M. Pasquale, J. Appl. Phys. **85**, 4361 (1999).

[22] K. Binder and A.P. Young, Rev. Mod. Phys. **58**, 801 (1986).